Monolayer hydrodynamics:

Coupling between bulk flow and insoluble monolayers at a gas/liquid interface

Amir H. Hirsa

Mechanical & Aerospace Engineering

Also Chemical & Biological Engineering
(joint appointment)

Rensselaer Polytechnic Institute

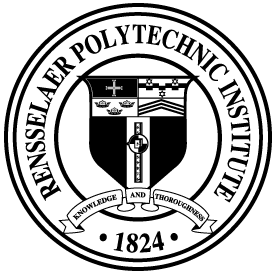

•On sabbatic at UCSB (office: Engineering-II, Room 3337, tel. x7346)
hirsaa@rpi.edu

Outline of Lectures

1) Macroscopic description of monolayers
    - A) Introduction to surfactant monolayers, including applications
    - B) Constitutive relation for Newtonian interface: Boussinesq-Scriven surface model and coupling to Navier-Stokes equations
    - C) Elastic and viscous response of monolayers: Why surfactant monolayers are elastic
    - D) Consequences of surface elasticity, including examples
2) Intrinsic interfacial viscosities: Not a figment of chemists' imagination
    - A) Surface shear viscosity
    - B) Surface dilatational viscosity
3) Monolayer mesoscale structure: Co-existing phase domains are common
    - A) Effect of co-existing phase domains on surface viscosities
    - B) Line tension between phase domains and inertia dominated flow
4) Monolayer phase morphology
    - A) Monolayer phase relaxation in the absence of flow
    - B) Effects of flow with inertia on co-existing phase domains
5) Monolayer measurements in flowing systems
    - A) Velocity measurements in free-surface boundary layers
    - B) Nonlinear optics measurements: Second-harmonic generation at gas/liquid interfaces
    - C) Free-surface microscopy: Laser-induced fluorescence microscope and Brewster angle microscope
6) Flow-induced protein crystallization: A biotech application
    - A) Two-dimensional protein crystallization
    - B) Flow-induced and flow-enhanced 2D protein crystallization at air/water interface
    - C) "One-dimensional" protein crystals induced by flow

Prevalence of gas/liquid interfaces

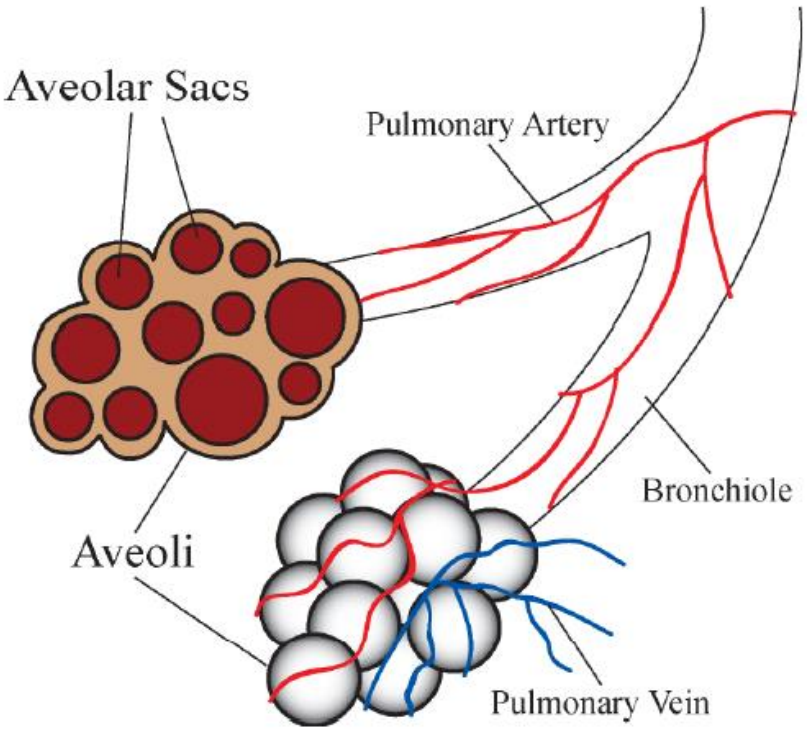

(a)

(b)

Figure 1.1: Examples of systems with gas/liquid interfaces: (a) The air/water interface inside the alveolar sacs of our lungs is essential for respiration. (b) Photograph of the Singapore river. The study of carbon dioxide exchange between the oceans and the air is an important topic in environmental research.

Motivation for studying monolayers in fluid flow and applications

- Monomolecular films (monolayers) are ubiquitous on water
- Small amounts can have big effects: They can significantly influence transport of mass, momentum and energy

Applications in traditional & emerging technologies:

- Manufacturing (e.g., foams, emulsifiers in food processing)
- Coating processes
- Fuel injection
- Microsystems (e.g., microfabrication, inkjets)
- Biological systems (e.g., lung surfactants)
- Environmental systems (e.g., CO_2 exchange)
- Sensors (bio-chemical)

An example from "Nature" Beer bubbles

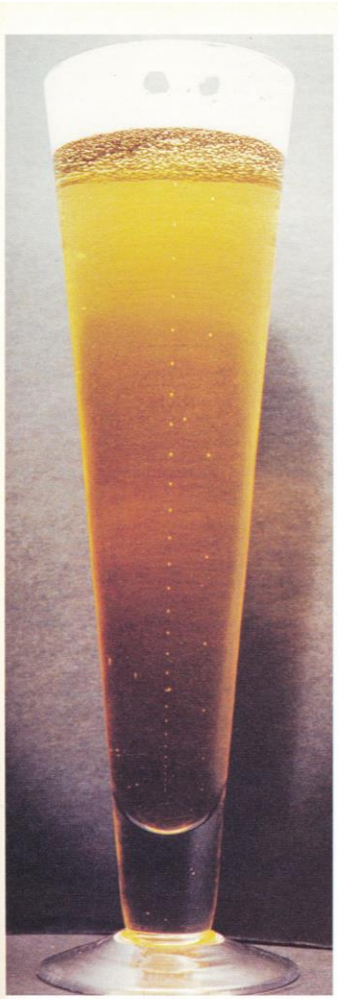

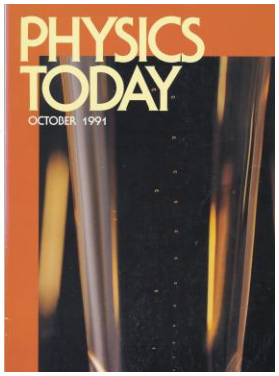

Bubbles in a glass of beer appear to rise in streams from spots on the surface of the glass. As they ascend, the bubbles grow larger and spread further apart. **Figure 1**

After a bottle of beer is opened, the partial pressure of dissolved CO_2 in the beer is greater than the pressure of the CO_2 in the bubble, and the dissolved gas travels from the beer to the bubble. Because this pressure difference remains almost constant, we expect (to a good approximation) the rate of bubble growth to be proportional to the surface area of the bubble:

$$\frac{dN_{bubble}}{dt} = \gamma(4\pi r^2) \qquad (1)$$

where N_{bubble} is the number of CO_2 molecules in the bubble, γ is a proportionality constant, and $4\pi r^2$ is the surface area, based on the assumption that the bubble is a sphere of radius r. The simple form of equation 1 is valid only because the beer maintains the bubble at constant temperature and the atmosphere maintains the bubble at a constant pressure (the hydrostatic pressure of the beer being negligible).

Assume the CO_2 in a beer bubble obeys the ideal gas law, so that $P_{bubble} V_{bubble} = N_{bubble} k_B T_{bubble}$, where k_B is the Boltzmann constant and P_{bubble}, V_{bubble} and T_{bubble} are the pressure, volume and temperature of the bubble. Because P_{bubble} and T_{bubble} are constant, we can differentiate both sides of the ideal gas law with respect to time to find

$$\frac{dN_{bubble}}{dt} = \left(\frac{P_{bubble}}{k_B T_{bubble}}\right)\frac{dV_{bubble}}{dt} = \left(\frac{P_{bubble}}{k_B T_{bubble}}\right)4\pi r^2 \frac{dr}{dt} \qquad (2)$$

If we set equation 1 equal to equation 2, we can solve the resulting first-order differential equation to find that

$$r = r_0 + v_r t \qquad (3)$$

where r_0 is the initial radius of the bubble and $v_r = \gamma k_B T_{bubble}/P_{bubble}$ is the rate of increase of the bubble's radius.

The stream of beer bubbles shown in figure 2 provides

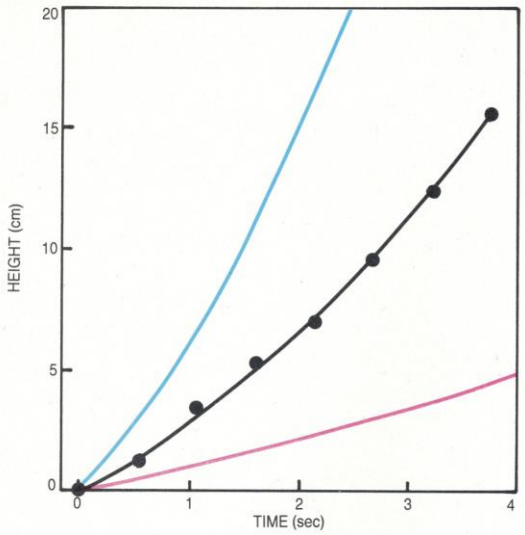

Height of a bubble in a glass of beer as a function of time, as determined from an enlarged version of figure 2. The data points are roughly one standard deviation in size. The black curve is the expected trajectory of a beer bubble if one assumes that the drag force F_d follows that of a rigid sphere with $r_0 = 0.0143$ cm and $v_r = 0.0042$ cm/sec. If one assumes the same values for r_0 and v_r but that the drag force follows either Stokes's law $F_d = 6\pi\rho v_z r$ (blue) or Oseen's law $F_d = 6\pi v_z r(1 + {}^3/_{16} R)$ (red), the calculated trajectories do not match the observed ones. **Figure 4**

Re ≈ 10

A high *Re* example from Nature Surface waves

clean

with monolayer
(~1 part in 10,000 by mass)

time

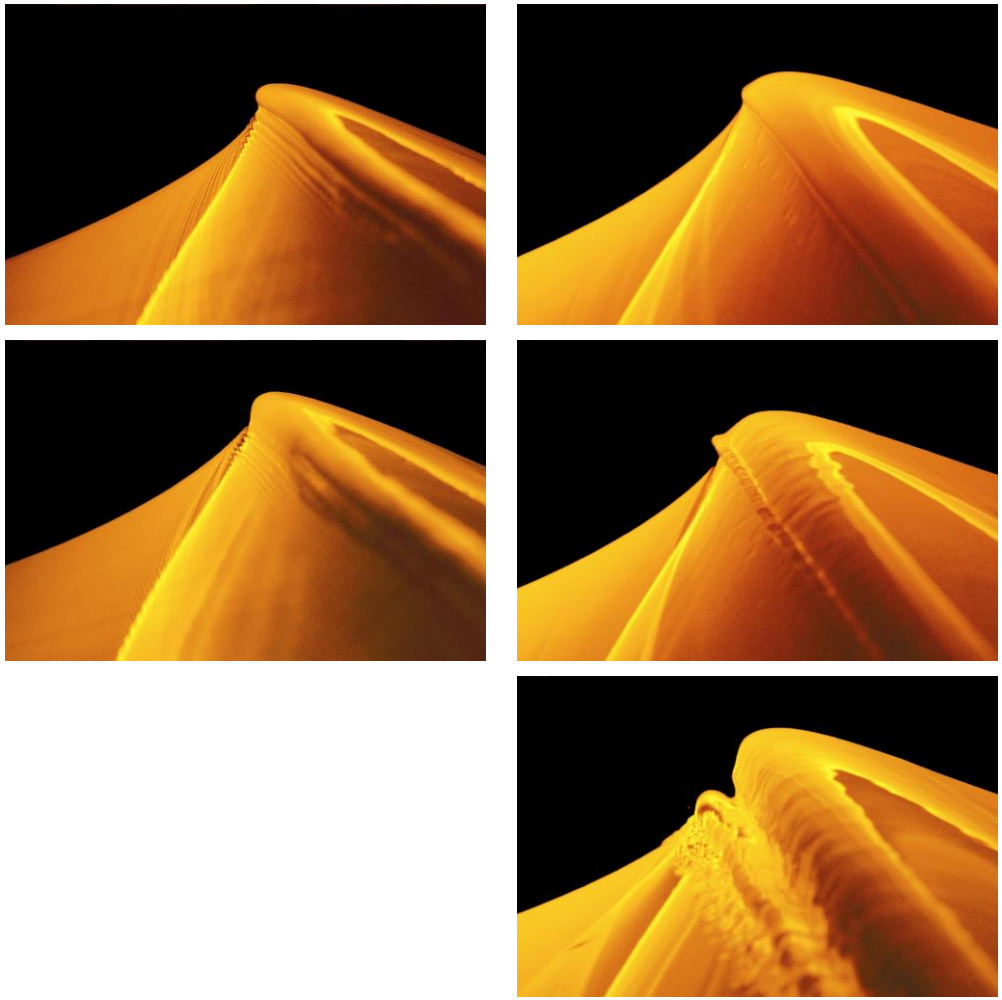

$Re_\lambda \approx 10^6$
($\lambda \approx 1$ m)

Liu & Duncan *Nature* (2003)

Examples from the laboratory

Bulk flow

$Re \approx 10^4$

(L ≈ 0.1 m)

clean

monolayer

(~1 milligram/m^2)

time

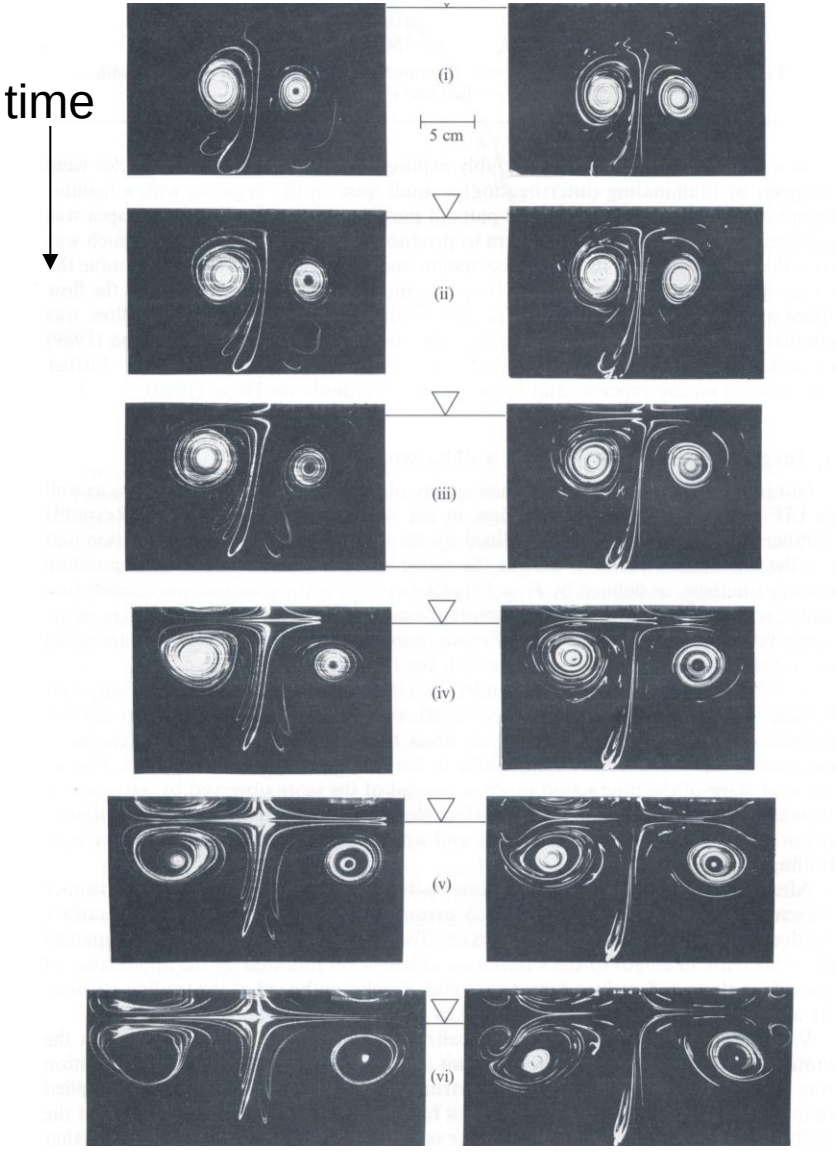

Hirsa & Willmarth *JFM* (1994)

A small scale example from the laboratory

Microfluidic pumping

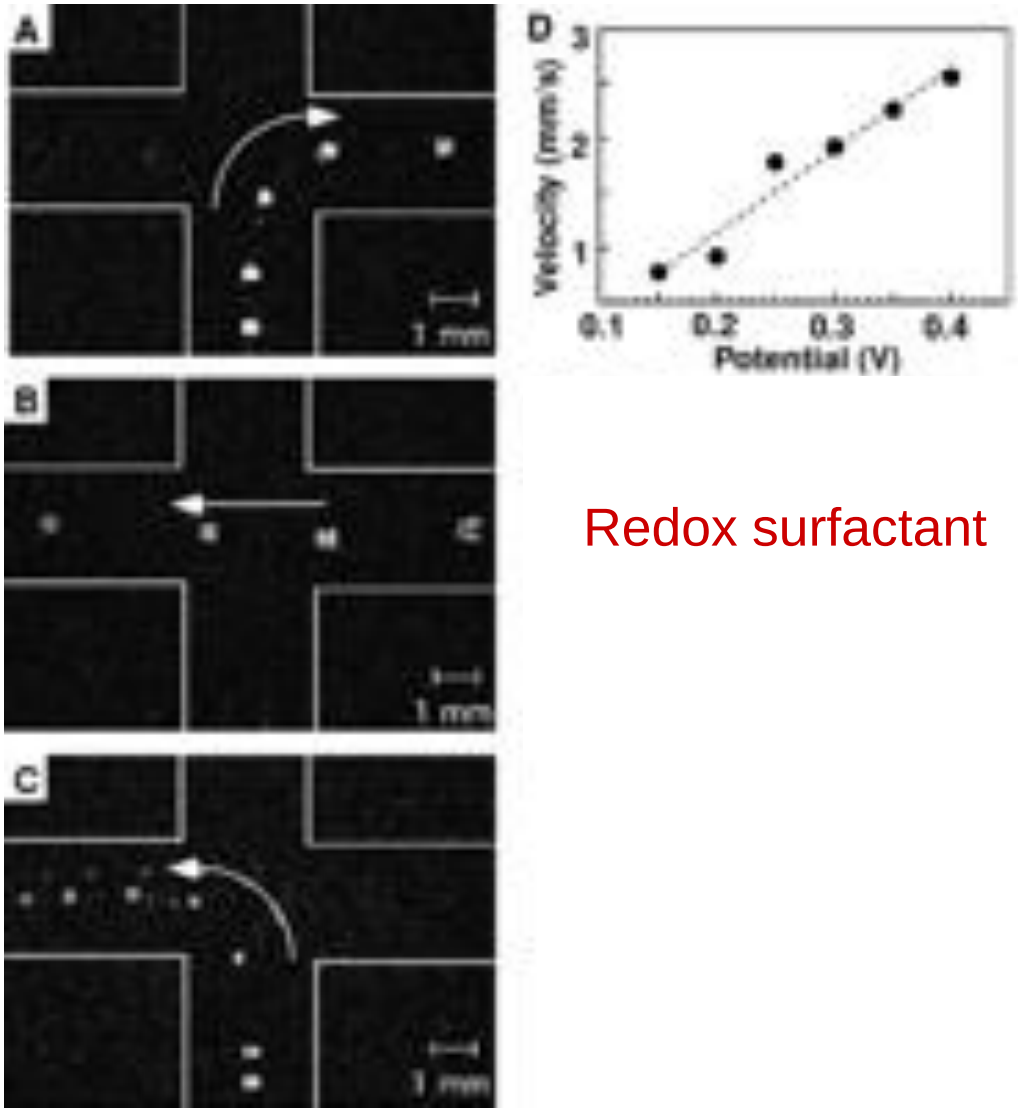

$Re \approx 10^{-1}$

Redox surfactant

Gallardo et al. *Science* (1999)

A “picture” of insoluble (Langmuir) monolayers

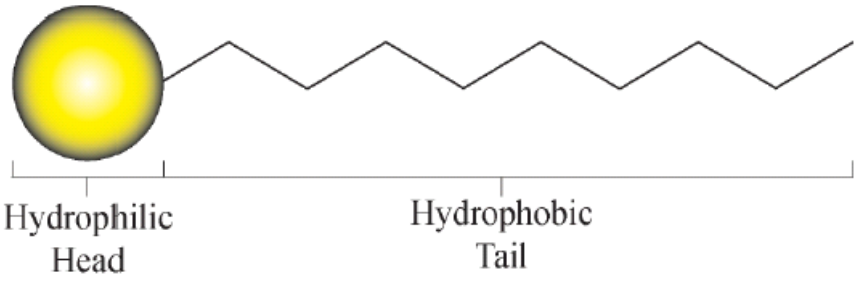

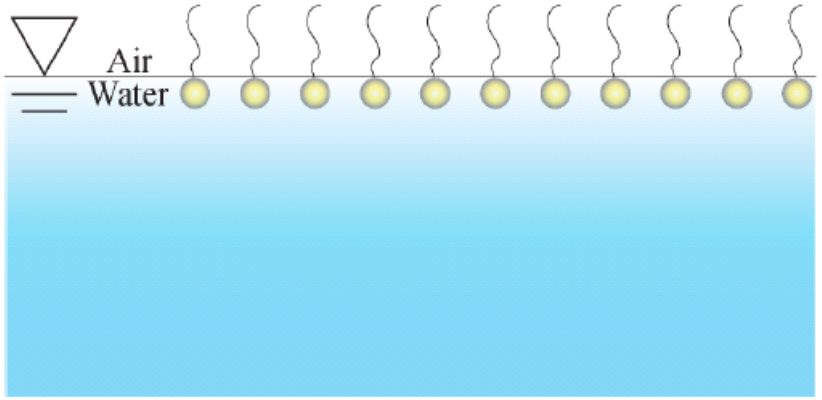

Note the amphiphilic nature of monolayer-forming materials

Boundary conditions for equations of motion

In the presence of surfactant monolayers, boundary conditions for Navier-Stokes equations are functions of intrinsic interfacial properties

For a Newtonian gas/liquid interface, the surface stress tensor is

$$\mathbf{T}^s = \sigma \mathbf{I}_s + \mathbf{S}^s = (\sigma + (\kappa^s - \mu^s)\, \mathrm{div}_s\, \mathbf{u}^s)\, \mathbf{I}_s + 2\, \mu^s\, \mathbf{D}^s\,,$$

where the viscous part of the surface stress tensor, $\mathbf{S}^s$, is a linear function of the surface rate of deformation tensor, $\mathbf{D}^s$

"Boussinesq-Scriven surface model"

Intrinsic interfacial properties:

1. σ thermodynamic (equilibrium surface tension)
2. μ^s surface shear viscosity
3. κ^s surface dilatational viscosity

e.g., for planar flow at flat interface, the x-component yields:

$$\mu \left.\frac{\partial u}{\partial y}\right|_{y=0} = \frac{\partial \sigma}{\partial x} + \frac{\partial}{\partial x}\left[\left(\kappa^s + \mu^s\right)\frac{\partial u^s}{\partial x}\right]$$

Background on Boussinesq-Scriven surface model

The Boussinesq-Scriven (B-S) equations for the surface are a direct analogy of the three dimensional Navier-Stokes (N-S) equations for a Newtonian fluid. The gradients of the stresses (neglecting body forces) acting on the bulk fluid in scalar form for N-S are as follows:

$$-\frac{\partial p}{\partial x}+\frac{\partial}{\partial x}\left(2\mu\frac{\partial u}{\partial x}+\lambda\,\mathrm{div}\,\boldsymbol{u}\right)+\frac{\partial}{\partial y}\left[\mu\left(\frac{\partial u}{\partial y}+\frac{\partial v}{\partial x}\right)\right]+\frac{\partial}{\partial z}\left[\mu\left(\frac{\partial w}{\partial x}+\frac{\partial u}{\partial z}\right)\right] \qquad (2.1)$$

$$-\frac{\partial p}{\partial y}+\frac{\partial}{\partial y}\left(2\mu\frac{\partial v}{\partial y}+\lambda\,\mathrm{div}\,\boldsymbol{u}\right)+\frac{\partial}{\partial x}\left[\mu\left(\frac{\partial v}{\partial x}+\frac{\partial u}{\partial y}\right)\right]+\frac{\partial}{\partial z}\left[\mu\left(\frac{\partial v}{\partial z}+\frac{\partial w}{\partial y}\right)\right] \qquad (2.2)$$

$$-\frac{\partial p}{\partial z}+\frac{\partial}{\partial z}\left(2\mu\frac{\partial w}{\partial z}+\lambda\,\mathrm{div}\,\boldsymbol{u}\right)+\frac{\partial}{\partial x}\left[\mu\left(\frac{\partial w}{\partial x}+\frac{\partial u}{\partial z}\right)\right]+\frac{\partial}{\partial y}\left[\mu\left(\frac{\partial v}{\partial z}+\frac{\partial w}{\partial y}\right)\right] \qquad (2.3)$$

Notation based on Schlichting

Similarly, the gradients of the surface stresses (neglecting body forces) acting on a 2D interface in scalar form for B-S are as follows:

$$\frac{\partial \sigma}{\partial x} + (\kappa^s + \mu^s) \frac{\partial}{\partial x} \left(\frac{\partial u^s}{\partial x} + \frac{\partial v^s}{\partial y} \right) + \mu^s \frac{\partial}{\partial y} \left(\frac{\partial u^s}{\partial y} - \frac{\partial v^s}{\partial x} \right)$$

$$\frac{\partial \sigma}{\partial y} + (\kappa^s + \mu^s) \frac{\partial}{\partial y} \left(\frac{\partial u^s}{\partial x} + \frac{\partial v^s}{\partial y} \right) - \mu^s \frac{\partial}{\partial x} \left(\frac{\partial u^s}{\partial y} - \frac{\partial v^s}{\partial x} \right)$$

Notation based on Edwards et al. (1991, p. 112) for a Newtonian interface (at z = constant)

the (bulk) stress tensor is:

λ (second coefficient of viscosity)

$$\boldsymbol{\tau} = \left(-p + \left(\mu' - \frac{2}{3}\mu\right)\right) \operatorname{div} \boldsymbol{u} + 2\mu\mathbf{D}$$

Note that the bulk viscosity, given by $\mu' = \lambda + \frac{2}{3}\mu$

The surface stress tensor is analogous and is given by:

$$\boldsymbol{T}^{\mathrm{s}} = \left(\sigma + \left(\kappa^{\mathrm{s}} - \mu^{\mathrm{s}}\right) \operatorname{div}_{\mathrm{s}} \boldsymbol{u}^{\mathrm{s}}\right) \mathbf{I}^{\mathrm{s}} + 2\mu^{\mathrm{s}} \mathbf{D}^{\mathrm{s}}$$

Comparison between the varibles and properties of bulk flow and surface flow

Flow Properties/Variables	Bulk	Surface
x-velocity	u	u^{s}
y-velocity	v	v^{s}
rate of deformation tensor	$\mathbf{D}$	$\mathbf{D}^{\mathrm{s}}$
pressure	p	$-\sigma$
coefficient of shear viscosity	μ	μ^{s}
coefficient of dilatational viscosity	μ'	κ^{s}

Isolating the elastic effect: Quasi-stagnant monolayer

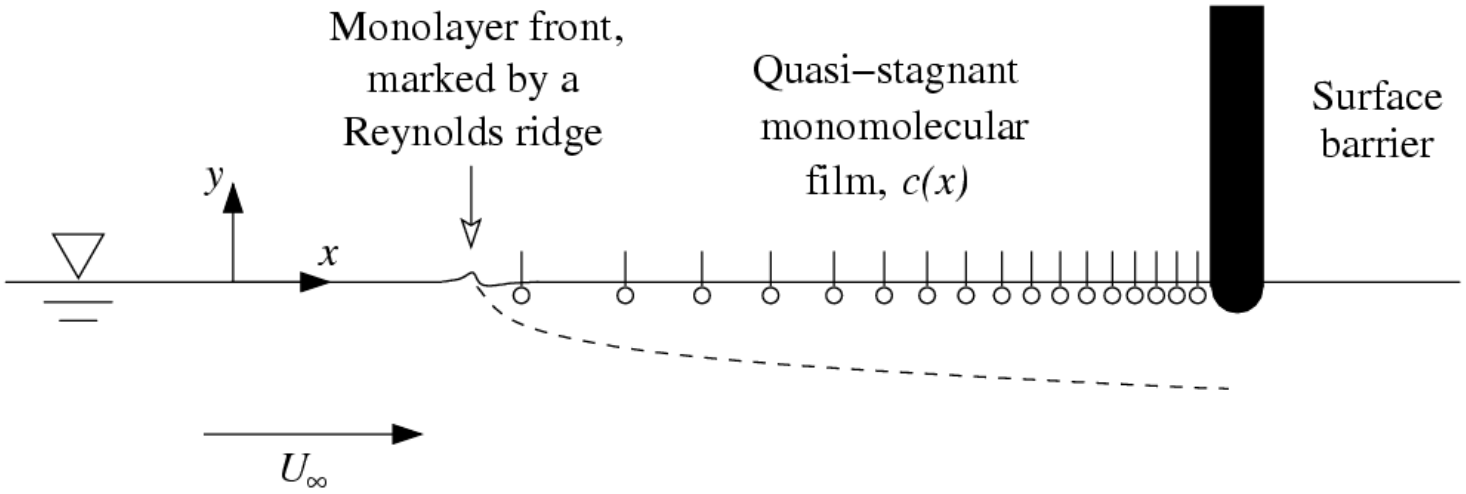

Note (undisturbed) interface at y = const.

Measured interfacial velocity & tangential stress

Interfacial velocity u^s

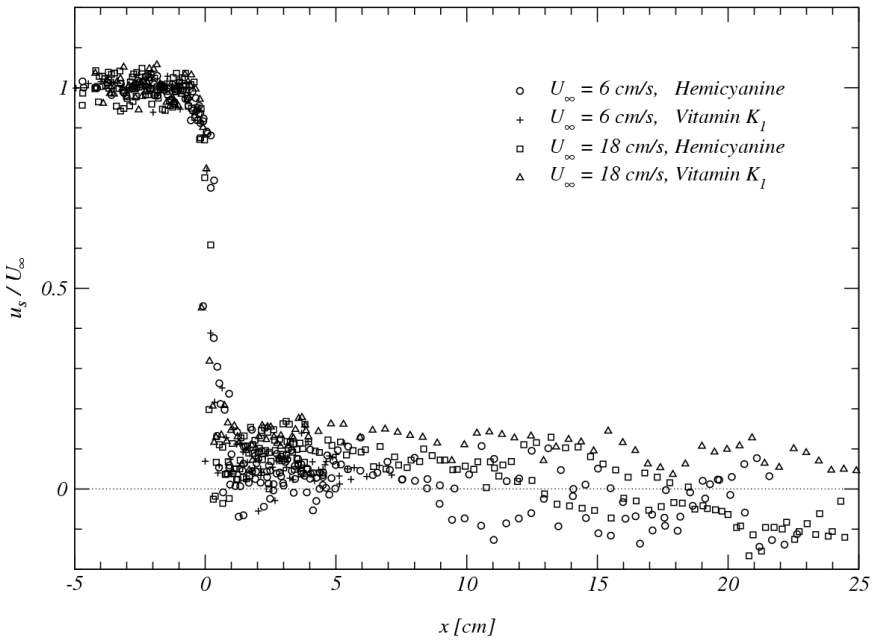

(tangential) shear at interface $\left.\frac{\partial u}{\partial y}\right|_{y=0}$

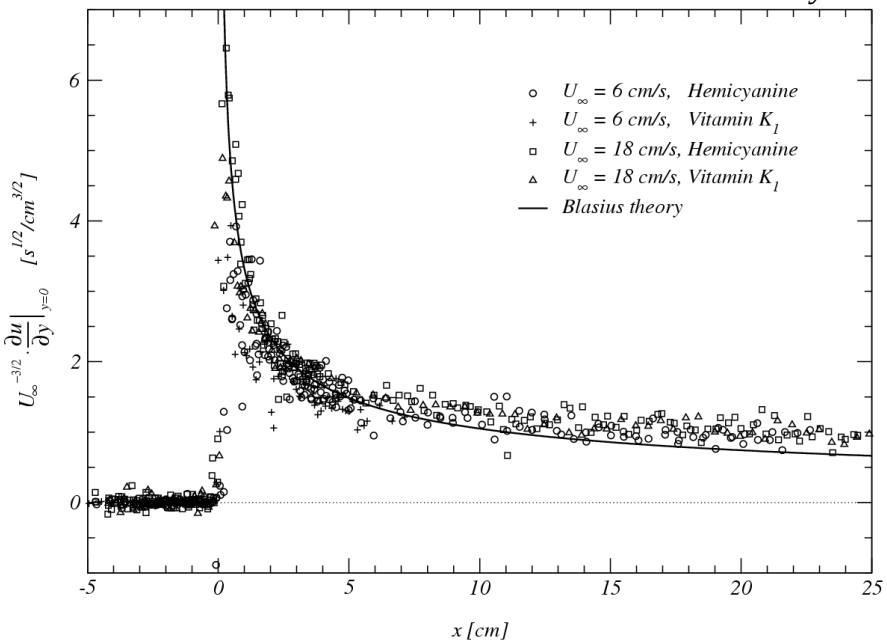

Notice the magnitude of the shear stress at the interface

Vogel & Hirsa *JFM* (2002)

Simultaneous measurements of velocity & concentration

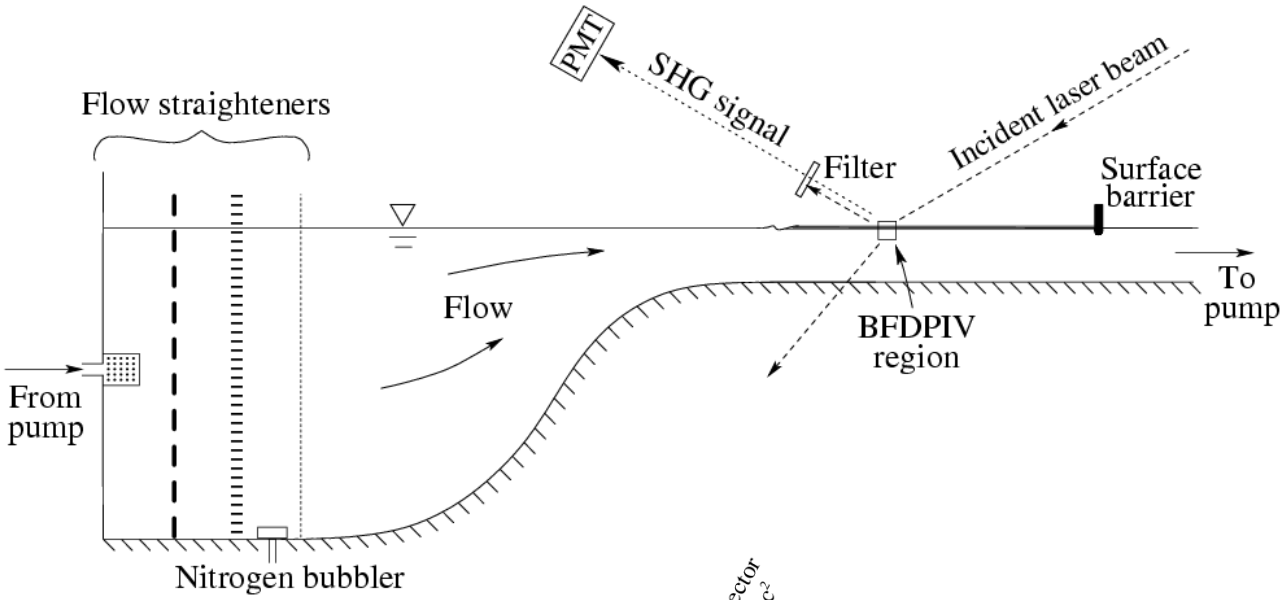

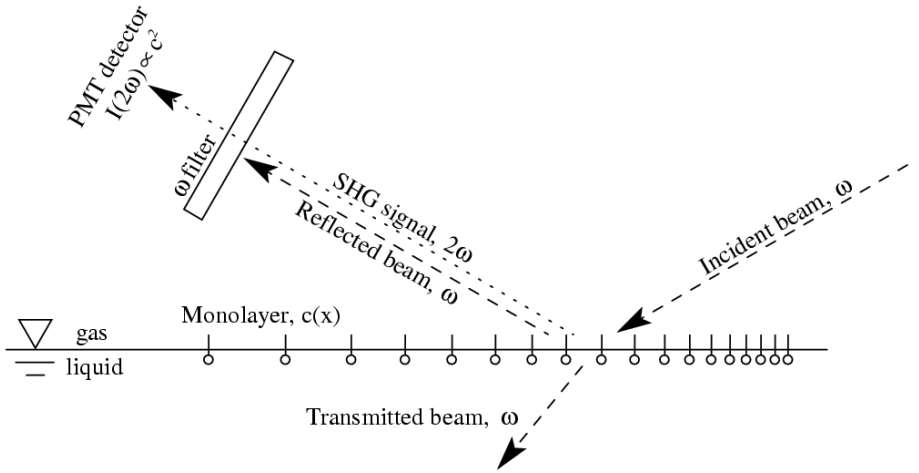

Vogel et al. *Rev Sci Inst* (2001)

Simple, elastic model (based on equation of state)

x-component of stress boundary condition for a fully viscoelastic interface:

$$\mu\left(\frac{\partial u}{\partial y}+\frac{\partial v}{\partial x}\right)=\frac{\partial \sigma}{\partial x}+(\kappa^s+\mu^s)\frac{\partial}{\partial x}\left(\frac{\partial u}{\partial x}+\frac{\partial w}{\partial z}\right)+\mu^s\frac{\partial}{\partial z}\left(\frac{\partial u}{\partial z}-\frac{\partial w}{\partial x}\right)$$

For a flat, quasi-stagnant interface reduces to:

$$\mu\left.\frac{\partial u}{\partial y}\right|_{y=0}=\frac{\mathrm{d}\sigma}{\mathrm{d}x}=\frac{\mathrm{d}\sigma}{\mathrm{d}c}\frac{\mathrm{d}c}{\mathrm{d}x}$$

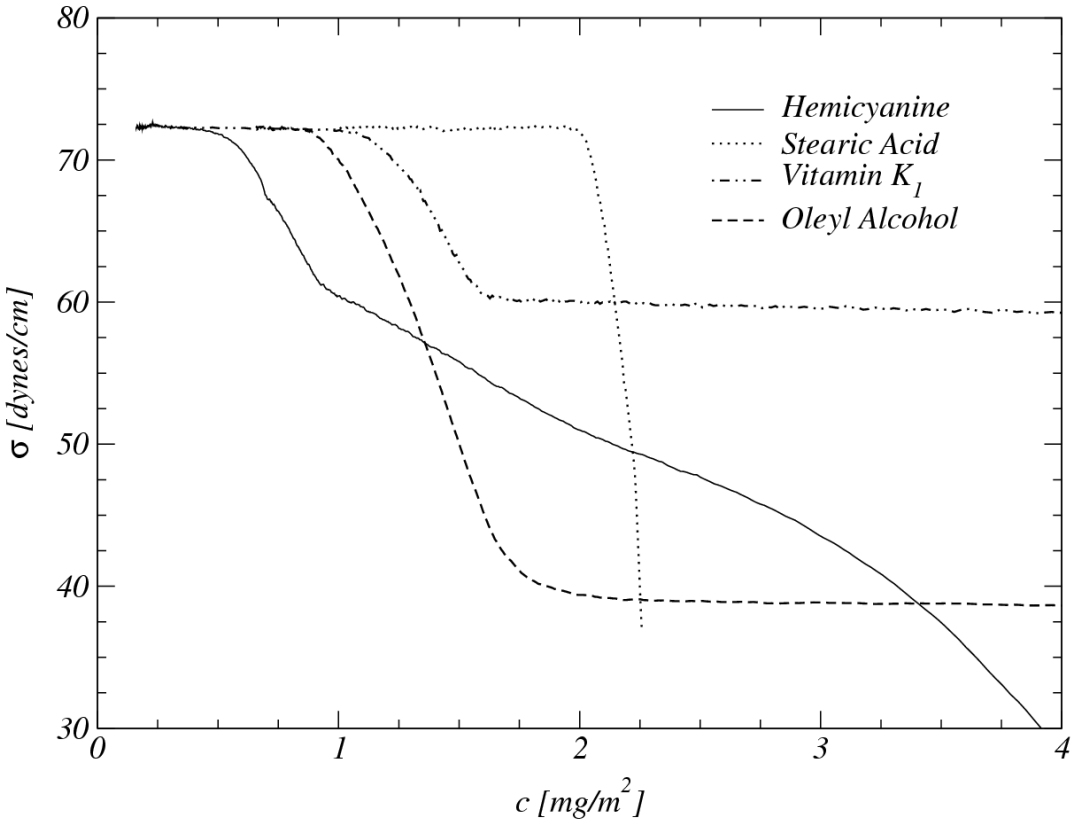

Monolayer concentration: measured (via SHG) vs. model

Hemicyanine

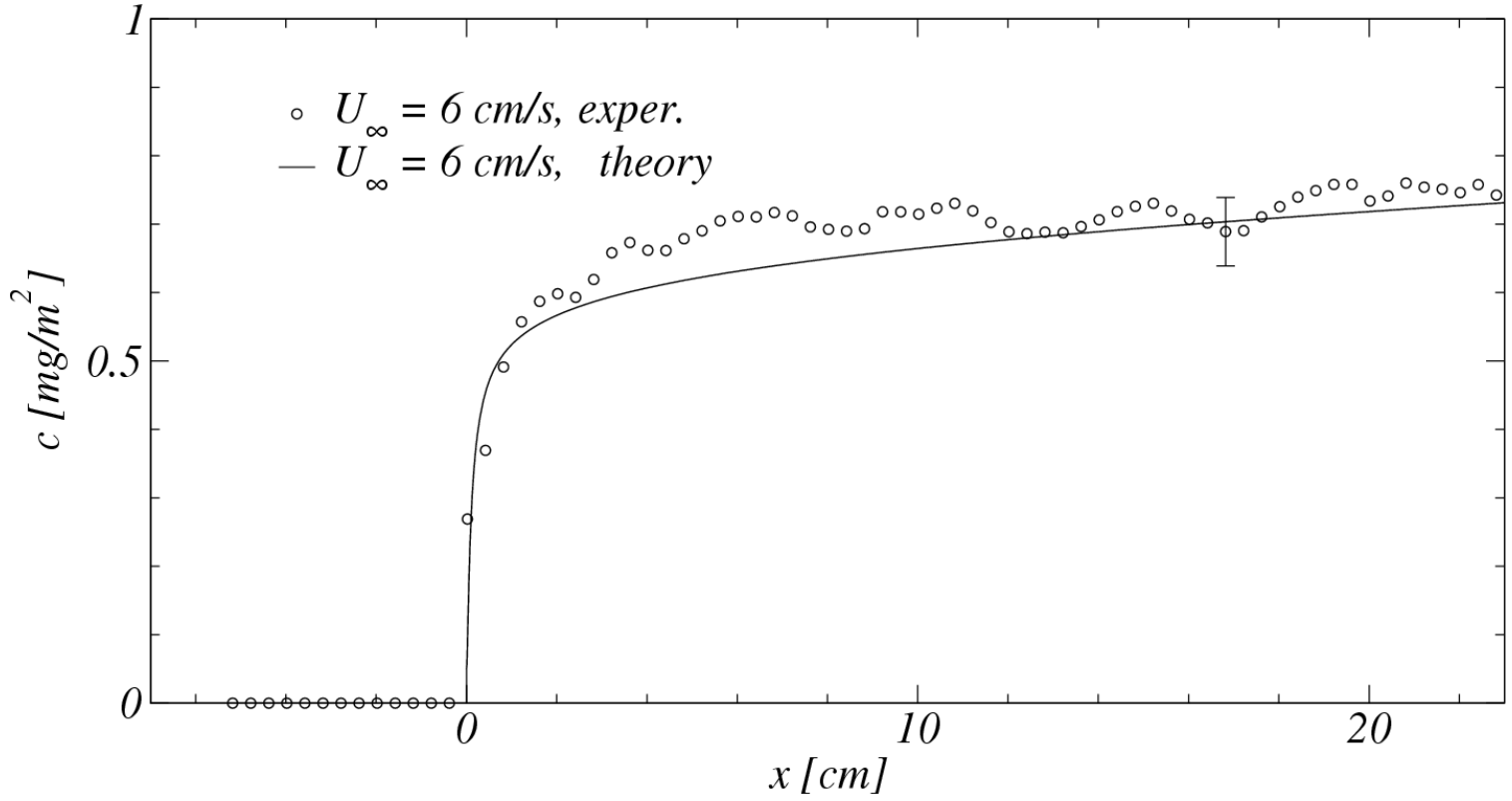

Vogel & Hirsa *JFM* (2002)

Film length: measured vs. model

Hemicyanine

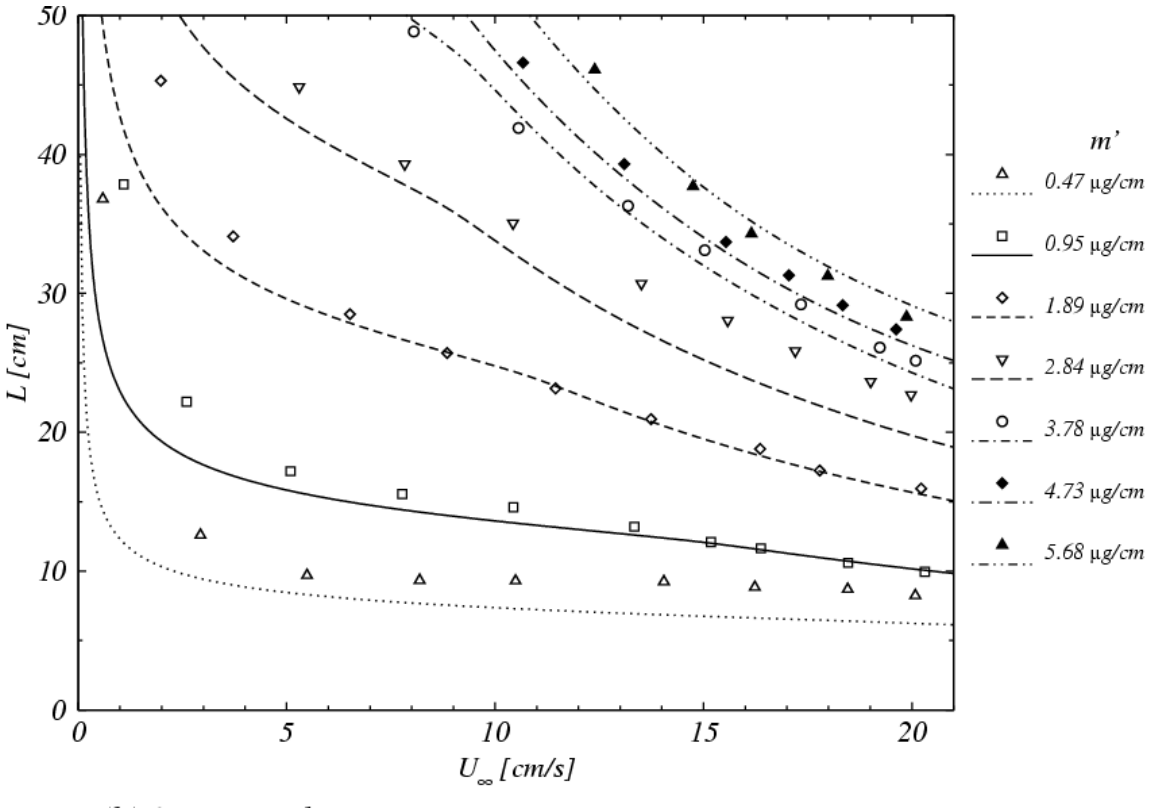

Vogel & Hirsa *JFM* (2002)

Role of nonlinear equation of state

Hemicyanine

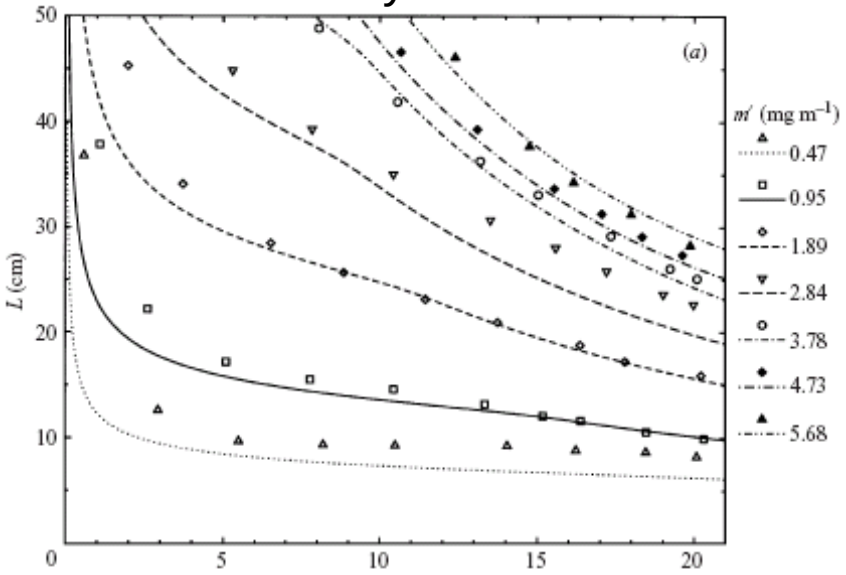

Vitamin K_1

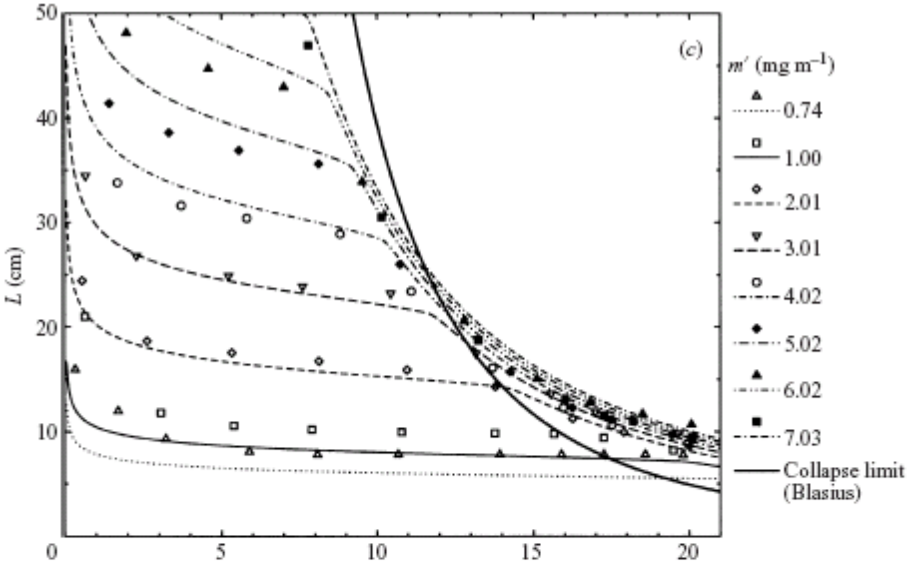

Stearic acid

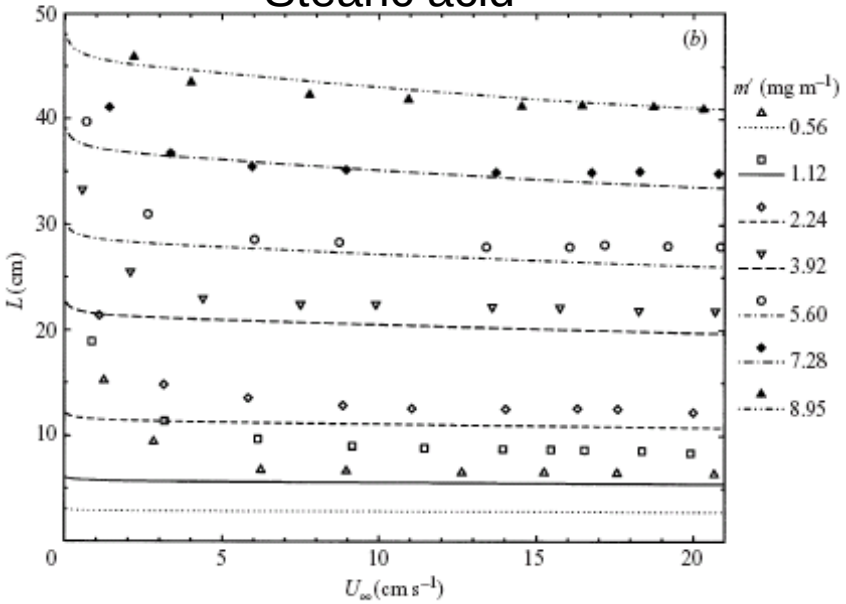

Oleyl alcohol

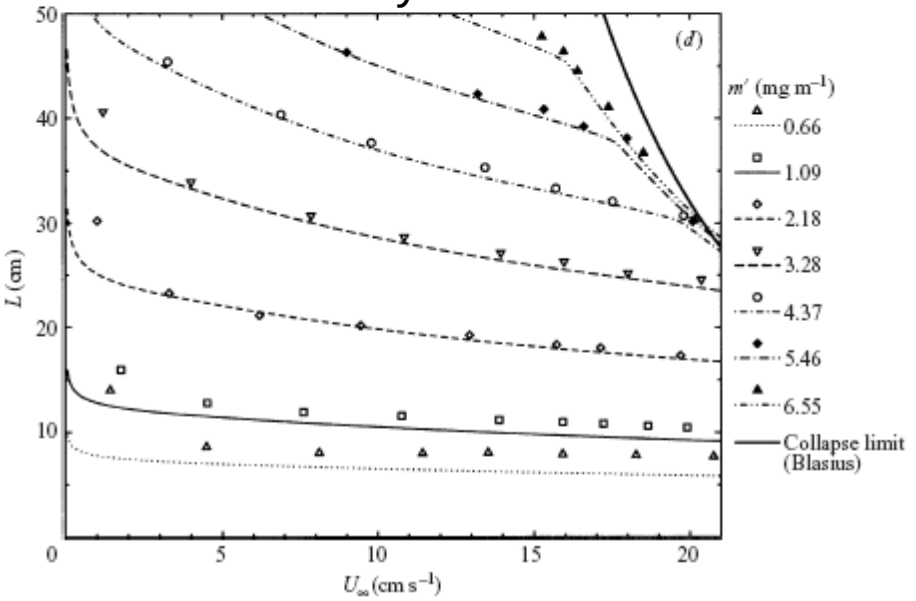

Deep-channel surface viscometer

(a more tractable geometry)

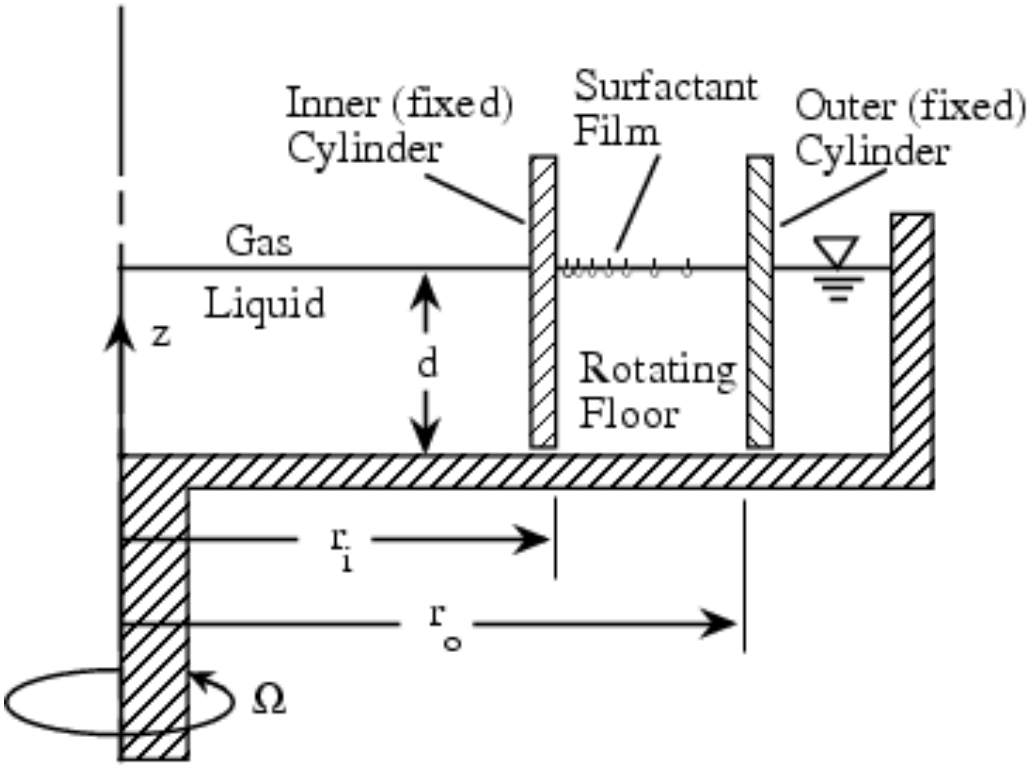

A monolayer (Vitamin K_1) with $\mu^s \approx 0$ was used, and steady flow (with inertia) is insensitive to κ^s effects, thereby isolating elastic effects, $\sigma(c)$

Computed flow field: vitamin K_1 (Re = 8,500)

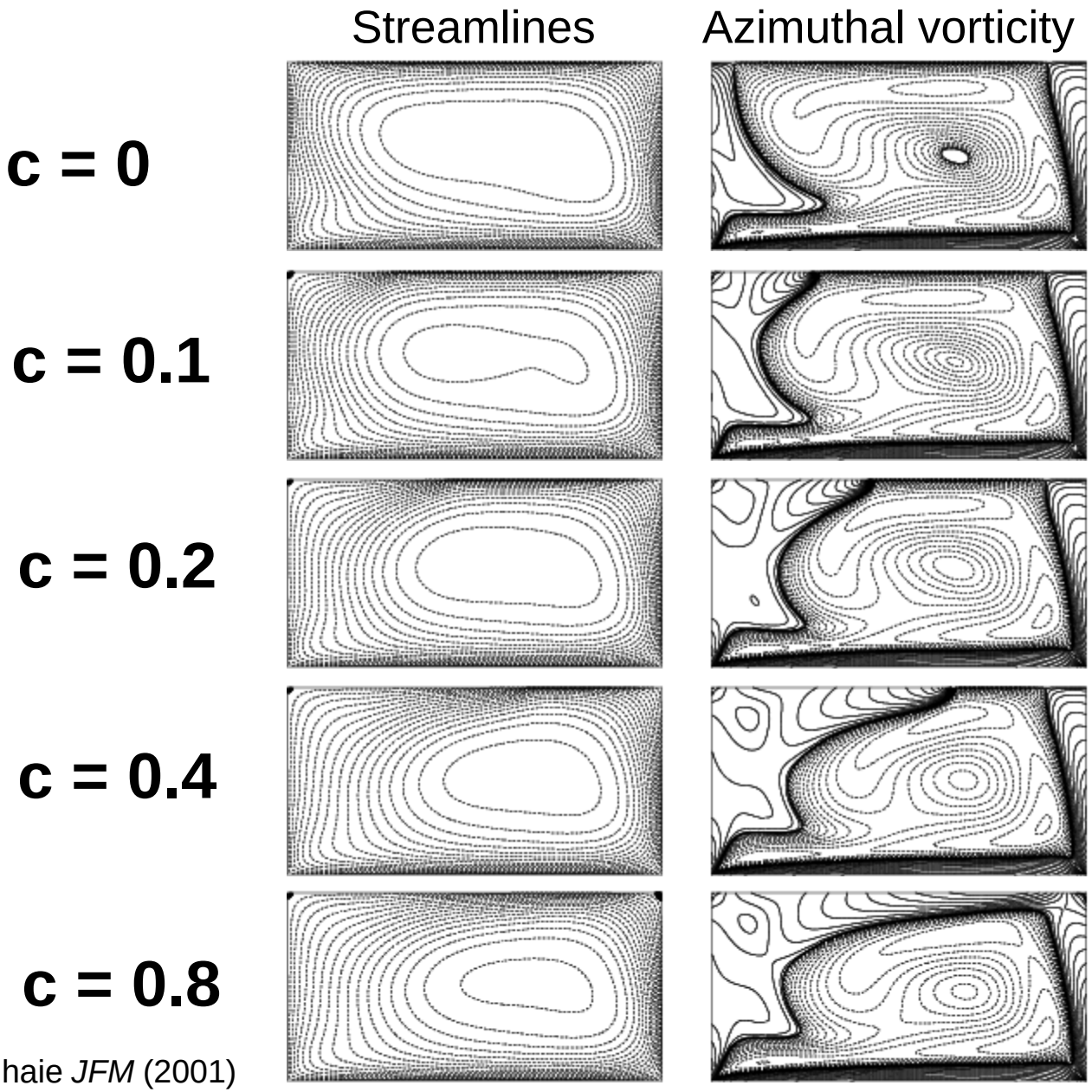

Hirsa, Lopez & Miraghaie *JFM* (2001)

Computed monolayer concentration distribution

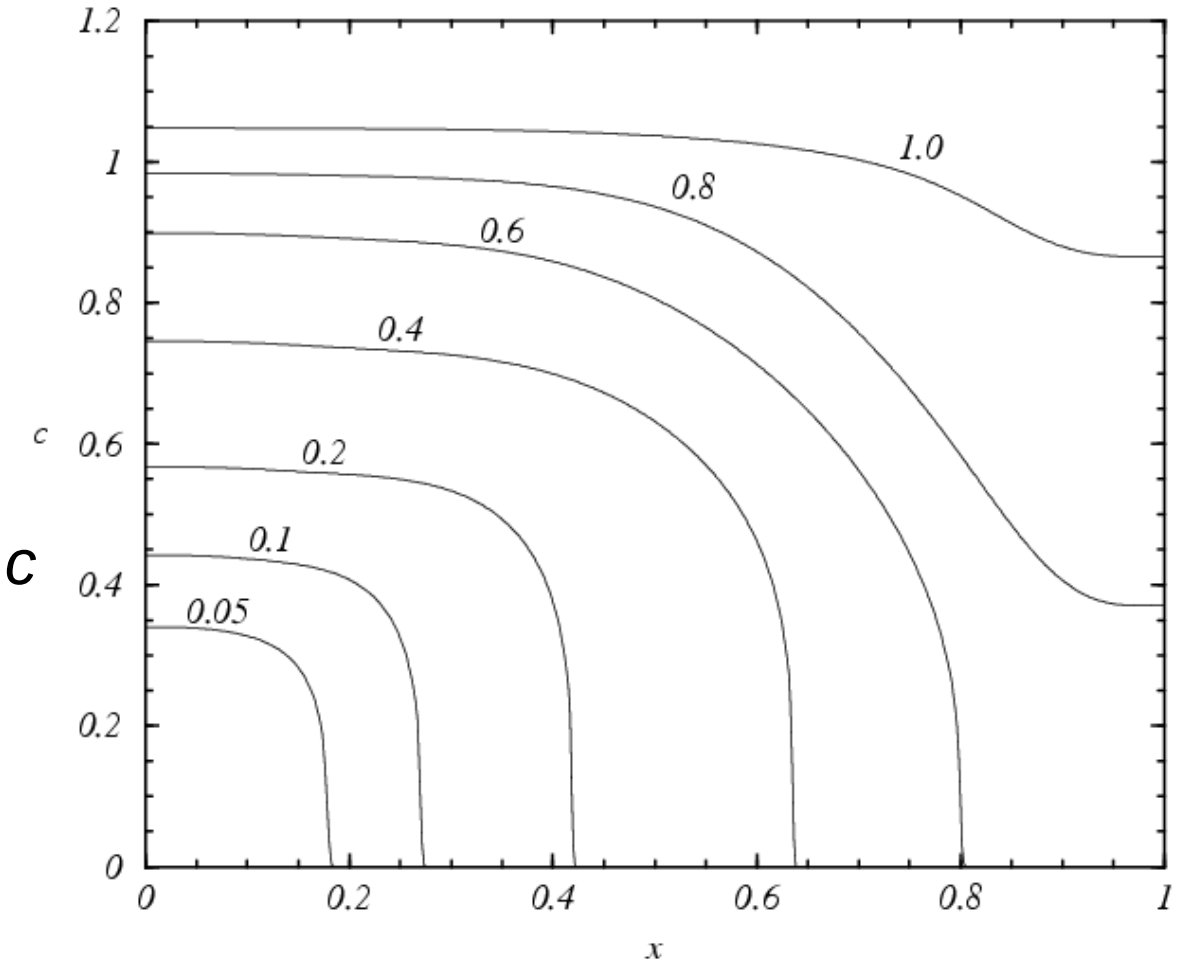

Hirsa, Lopez & Miraghaie *JFM* (2001)

Computed velocity distribution

Radial velocity

Azimuthal velocity

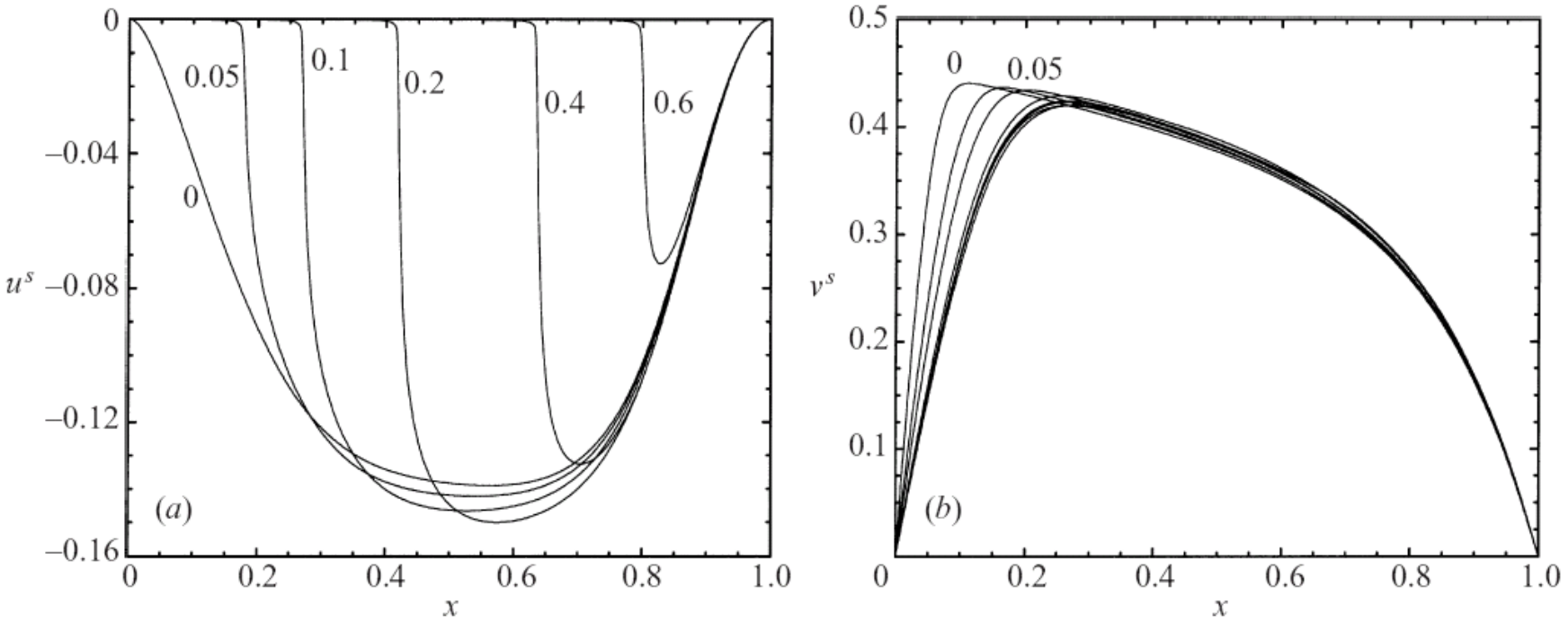

FIGURE 12. Computed profiles of (*a*) radial velocity at the interface, $u^s(x)$, and (*b*) azimuthal velocity at the interface, $v^s(x)$, for c_0 as indicated, at steady state for $Re = 8500$. In (*b*) for $c_0 > 0.2$ all profiles essentially collapse.

Hirsa, Lopez & Miraghaie *JFM* (2001)

Experimental apparatus

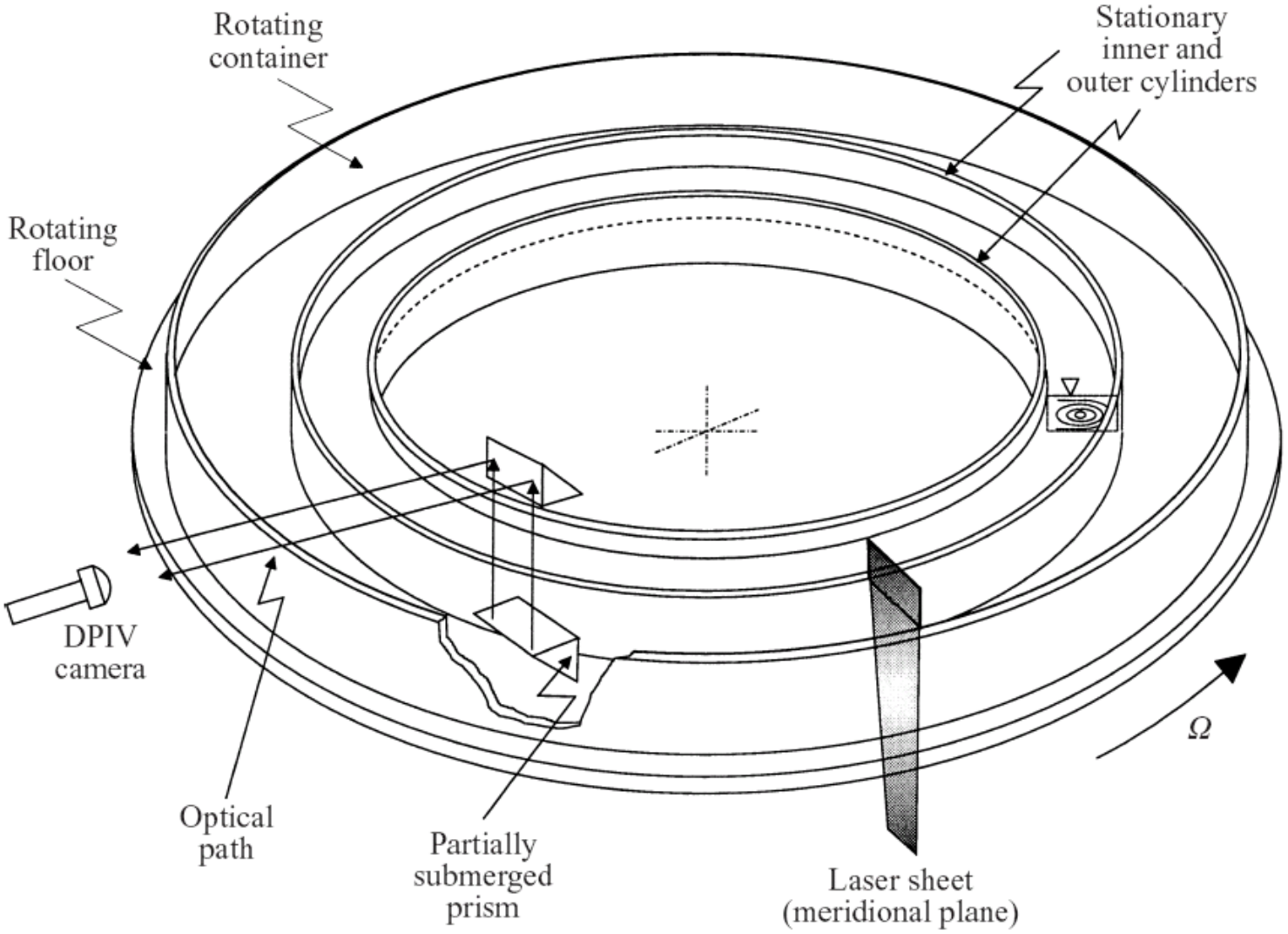

Surface velocity: measured vs. computed c = 0 (clean) or small c_0

Vitamin K_1

surface radial velocity u^s

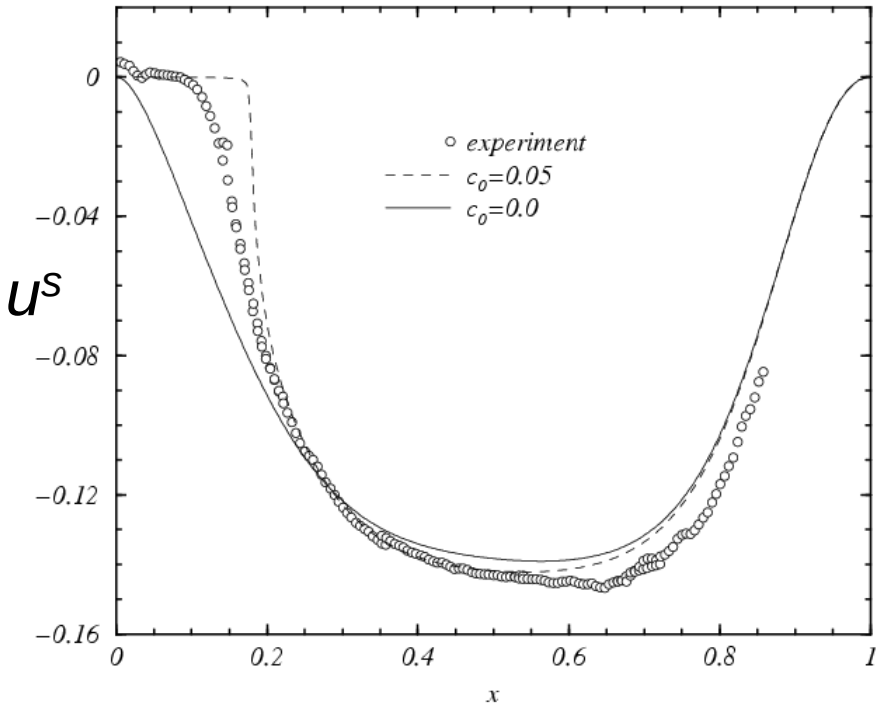

surface azimuthal velocity v^s

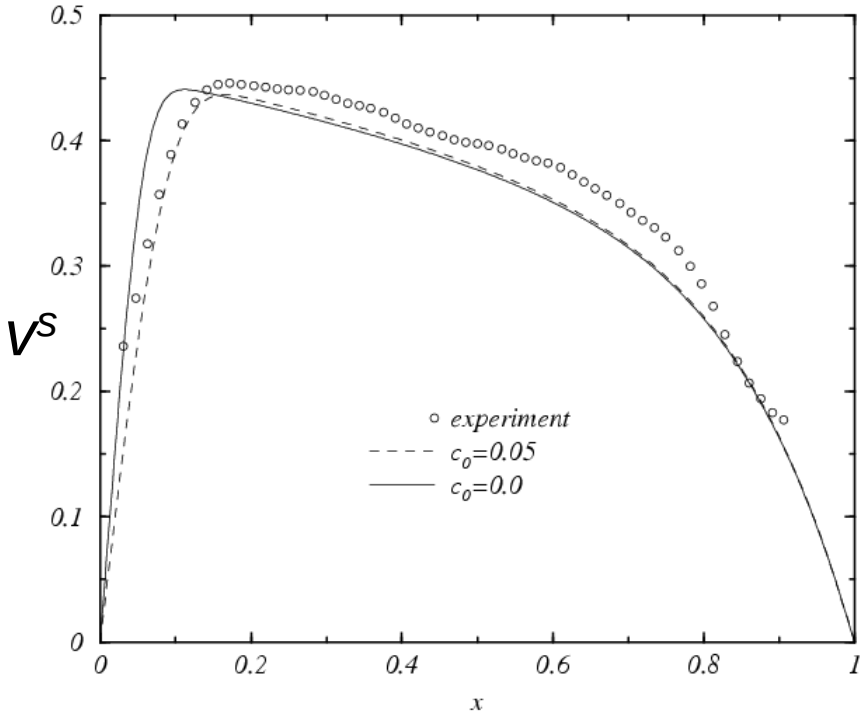

Hirsa, Lopez & Miraghaie *JFM* (2001)

Measured radial velocity for various c_o

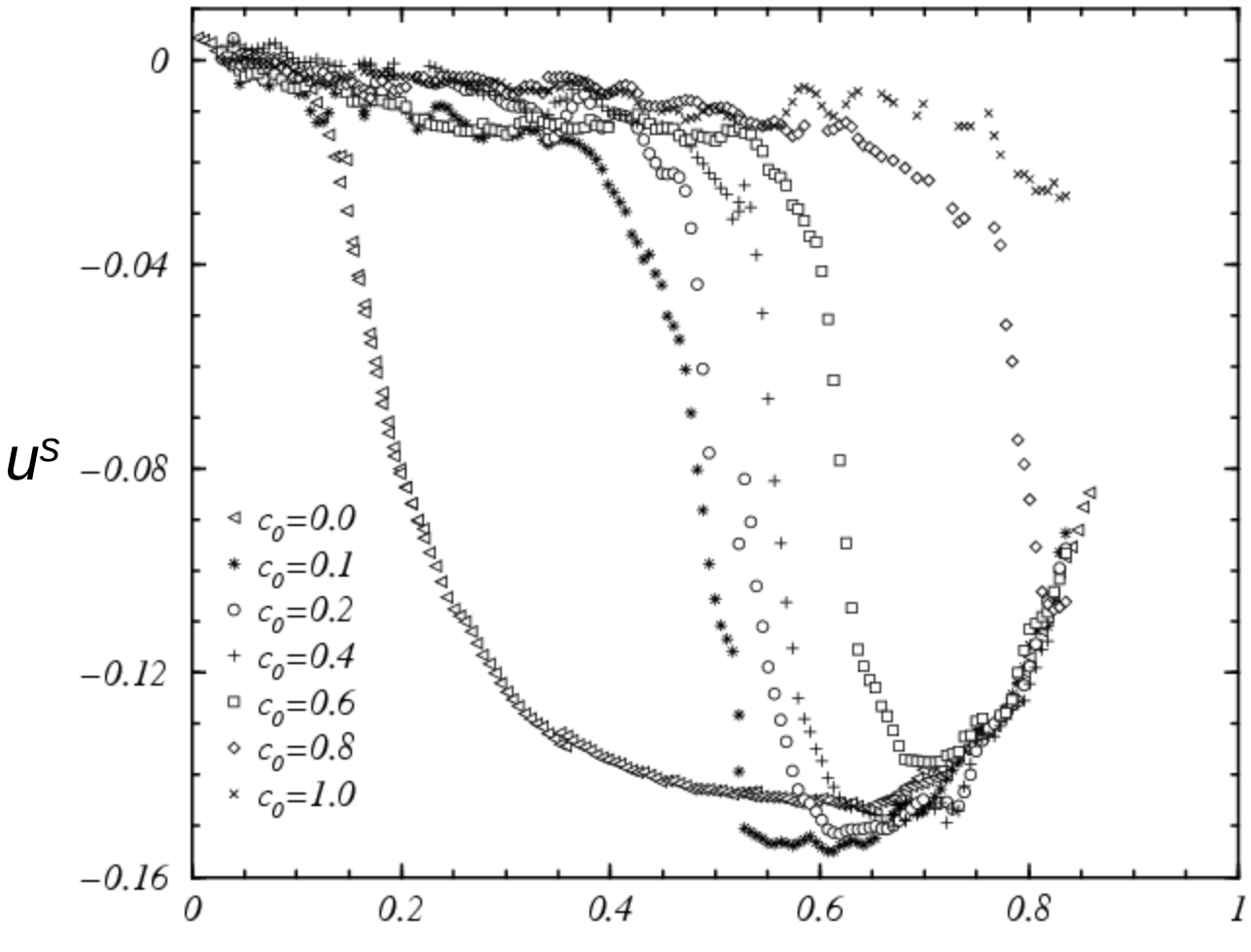

Discrepancy against computations due to small capillary number *Ca* = $\mu\Omega r_o/\sigma_o = 10^{-3}$

$$\eta^s = \frac{1}{Ca}\frac{\partial\bar{\sigma}}{\partial r}$$

Measured azimuthal velocity for various c_o

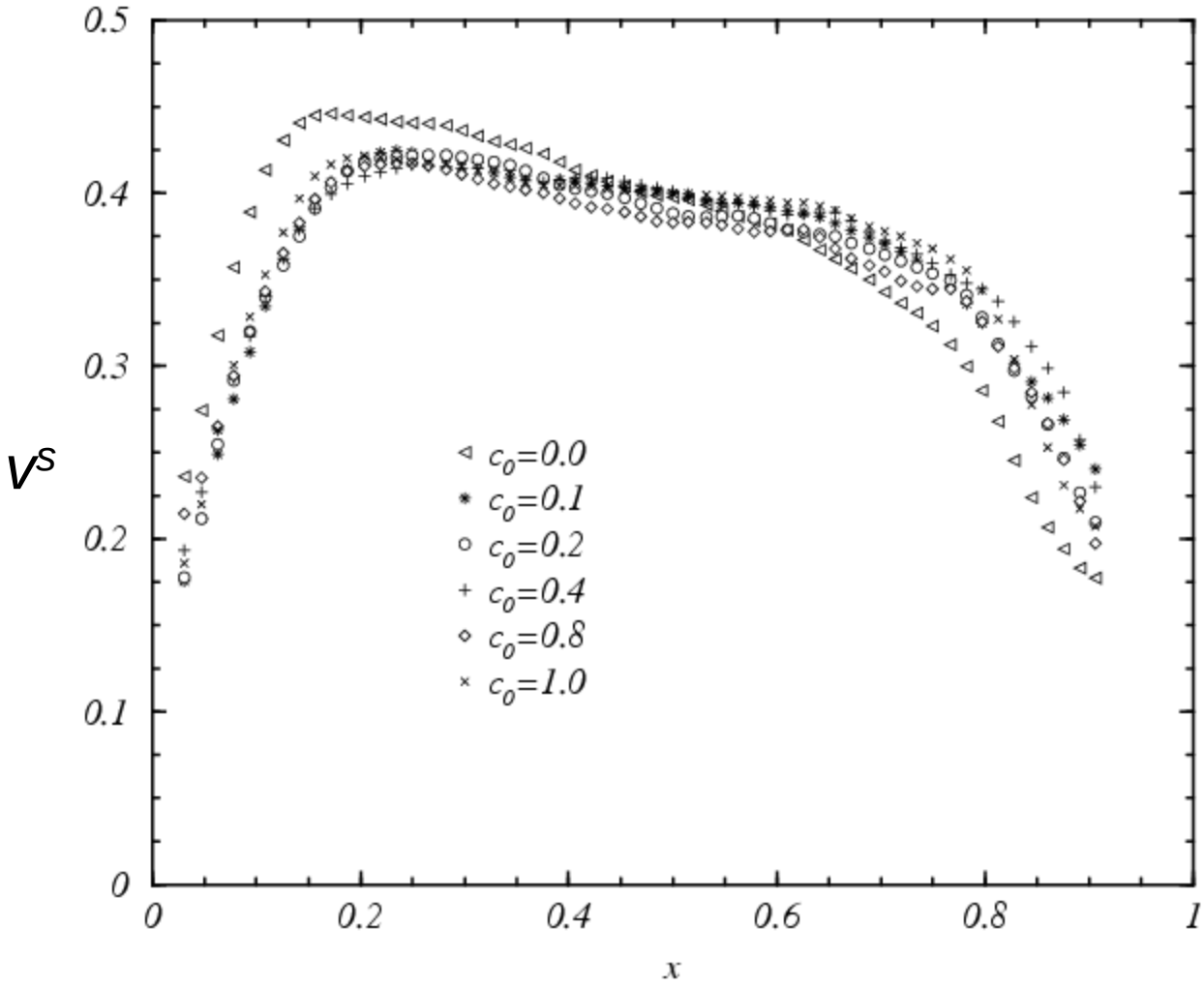

Boussinesq-Scriven surface model: $\sigma(c)$ understood for simple systems and works well as a macroscopic description

However, soluble systems, including proteins represent major challenges

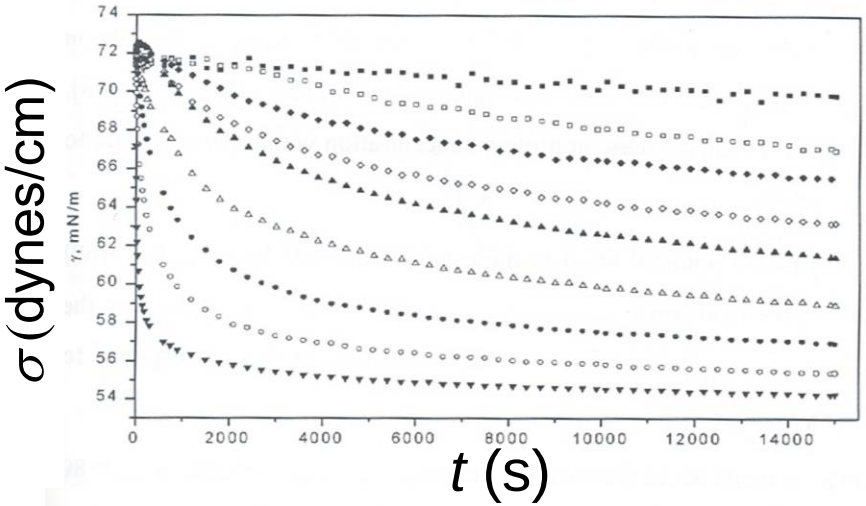

Fig. 14 Dynamic surface tension of HSA solutions at different initial bulk concentrations: $2\cdot10^{-8}$ (■), $3\cdot10^{-8}$ (□), $5\cdot10^{-8}$ (◆), $7\cdot10^{-8}$ (✧), 10^{-7} (▲), $2\cdot10^{-7}$ (Δ), $5\cdot10^{-7}$ (●), 10^{-6} (○), 10^{-5} mol/l (▼).

Fainerman & Miller (in Proteins at Liquid Interfaces 1998)

Next time…..

Boussinesq-Scriven surface model: μ^S

Clean interface
or
monolayer with small μ^S

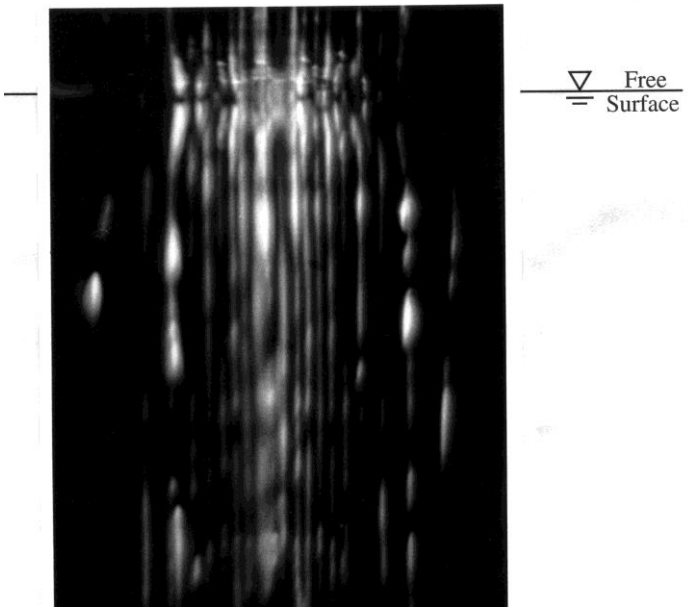

monolayer with large μ^S

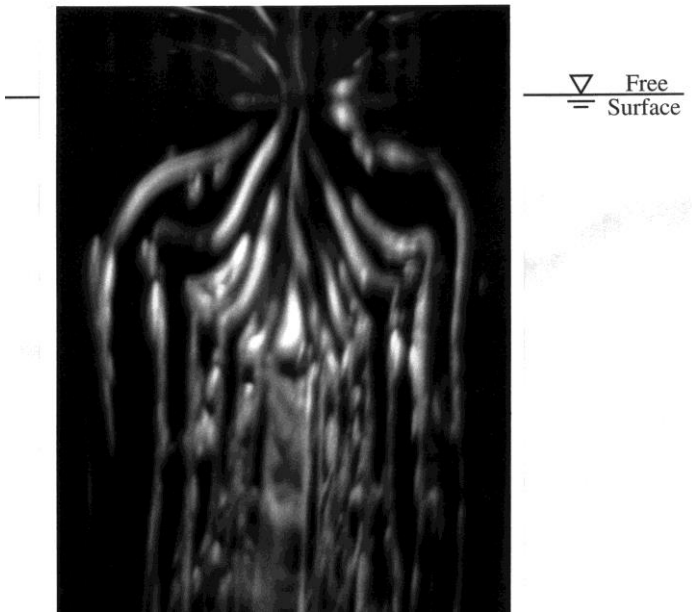

Hirsa, Harper & Kim *Phys Fluids* (1995)

Acknowledgements

Prof. Juan M. Lopez (Arizona State)

Dr. Michael J. Vogel (RPI, Cornell)

Dr. Reza Miraghaie (RPI, UCLA)

Dr. Jonathan Leung (RPI)

Research funded by: NSF (CTS)

Seminar series sponsored by Los Alamos National Laboratories through the Institute for Multiscale Materials Studies UCSB (Directed by Prof. Bud Homsy)